Virology 537 (2019) 254–262

Contents lists available at ScienceDirect

Virology

journal homepage: www.elsevier.com/locate/virology

PARP-1 mediated cell death is directly activated by ZIKV infection

Gang Xu[a,*,1], Shihua Li[b,1], Xinyuan Liu[b,c], Ping Gao[b], Xiaotong Chen[b], Haiyan Wang[a], Mingxia Zhang[a], Yang Yang[a], George Fu Gao[a,b], Fuping Zhang[a,b,**]

[a] Guangdong Key Laboratory for Diagnosis and Treatment of Emerging Infectious Diseases, Shenzhen Third People's Hospital, Shenzhen, 518112, China
[b] CAS Key Laboratory of Pathogenic Microbiology and Immunology, Institute of Microbiology, Chinese Academy of Sciences (CAS), Beijing, 100101, China
[c] University of Chinese Academy of Sciences, Beijing, 100049, China

ARTICLE INFO

Keywords:
Zika virus
PARP-1
NS3
Programmed cell death
NAD^+

ABSTRACT

Zika virus (ZIKV) has emerged as a severe health threat due to its association with microcephaly. It has been reported that the strong cytopathic effects, including cell-cycle arrest and cell death are responsible for the nervous system disease. However, the mechanisms by which ZIKV infection induced cell death were largely unknown. Here, we reported that cell death is readily detected after ZIKV infection as indicated by PI staining and the reduction of cell viability. Importantly, cell death can be induced by overexpression of ZIKV NS3 protein alone but not the other non-structure proteins. Mass spectrometry analysis revealed that NS3 bond to and activated PARP-1. In agreement with these observations, we found that PARP-1 was massively activated during ZIKV infection and the intracellular ATP and NAD^+ concentrations rapidly declined. Finally, PARP-1 knockdown simultaneously restrained ZIKV infection-induced cell death and ablated host restriction of virus infection. Our finding indicates that PARP-1 activation is an important cellular event during ZIKV infection, which contributes to the cell death.

1. Introduction

ZIKV, a mosquito-borne RNA virus, was first isolated in the Zika forest near Entebbe, Uganda in 1947 from a febrile sentinel rhesus monkey(Dick et al., 1952; Wikan and Smith, 2016; Zanluca and Dos Santos, 2016). It belongs to the Flavivirus genus, which include dengue (DENV), yellow fever (YFV), West Nile (WNV) and Japanese encephalitis (JEV)(Chambers et al., 1990). Similar to other flaviviruses, ZIKV contains a 10.7 kb genome, encoding a single polyprotein which can be cleaved by viral and host proteases into 3 structural proteins [capsid protein(C), membrane protein (M), envelope protein(E)] and 7 nonstructural proteins (NS1, NS2A, NS2B, NS3, NS4A, NS4B and NS5) (Li et al., 2017). NS5 and NS3 reside in the functional center for virus replication: NS5 is a RNA-dependent RNA polymerase (RdRp) required for genome replication, NS3 possesses protease activity (with cofactor NS2B) for polyprotein cleavage and helicase activity for unwinding dsRNA proceeding replication(Mottin et al., 2017; Saw et al., 2017).

ZIKV infection was neglected for many years since it was considered self-limiting with no long-term sequelae(Simpson, 1964). However, recent human cases and studies in mice have highlighted the role of ZIKV infection in neonatal birth defects. During the epidemic in Brazil, ZIKV infections during pregnancy have been linked to fetal malformations such as spontaneous abortion and microcephaly (Sarno et al., 2016; Ventura et al., 2016). This growing public health crisis raises the urgent need of a better understanding of the pathogenesis of ZIKV. It has been reported that ZIKV could efficiently target human neural progenitor cells (hNPCs) and brain organoids to induce cell death, providing a potential cause for microcephaly(Gaburro et al., 2018; Ghouzzi et al., 2016; Oh et al., 2017). However, the mechanism by which ZIKV infection induces cell death are largely unknown.

Programmed cell death (PCD) is a key mechanism of the innate immune system to protect against infection(Upton and Chan, 2014). Apoptosis, necroptosis and pyroptosis are well known mechanisms of programmed cell death which can be triggered by virus proteins, nucleic acid or even the cytokines induced by virus (Galluzzi et al., 2014; Häcker, 2018; Shi et al., 2017). Apoptosis is executed by a group of intracellular cysteine proteases, namely caspases(Häcker, 2018). Necroptosis is another form of regulated cell death mediated by the RIPK1-RIPK3-MLKL complex(Galluzzi et al., 2014). Pyroptosis occurs when caspase-1 is activated, leading to gasdermin D cleavage(Shi et al.,

* Corresponding author.
** Corresponding author. Guangdong Key Laboratory for Diagnosis and Treatment of Emerging Infectious Diseases, Shenzhen Third People's Hospital, Shenzhen, 518112, China.
E-mail addresses: xugang2513@sina.com (G. Xu), zhangfp@im.ac.cn (F. Zhang).
[1] These authors contributed equally.

https://doi.org/10.1016/j.virol.2019.08.024
Received 13 March 2019; Received in revised form 3 August 2019; Accepted 23 August 2019
Available online 25 August 2019

2017). In addition to the above PCD, recent studies report a new type of programmed cell death which is mediated by PARP-1(Andrabi et al., 2006; Koh et al., 2005; Wang et al., 2016; Yu et al., 2002). PARP-1 is a Poly(ADP-ribose) (PAR) polymerase highly expressed in the nucleus which catalyzes PAR synthesis using NAD^+ as a substrate and transfers the PAR onto various substrates to generate a branched PAR chain (Kraus and Hottiger, 2013). The process is named poly(ADP-ribosyl) ation (PARylation), and may alter the physical-chemical characteristics of the substrate with functional consequences (Kim et al., 2005; Shieh et al., 1998). PARP-1 is known to be implicated in DNA repair, transcription regulation, genome stability and apoptosis (Kim et al., 2005). PARP-1 has also been shown to regulate genome stability and DNA repair by PARylation of histones and the recruitment of single-strand DNA repair enzymes(Bouchard et al., 2003). However, excessive activation of PARP-1 can cause cell death as evidenced by the observation that deletion of the *parp-1* gene or PARP-1 inhibitors can suppress cell death(Yu et al., 2002). The mechanism by which PARP-1 mediates cell death has become clearer with the theory that NAD^+ and ATP are used up by massive PARP-1 activation which ultimately leading to cell death by energy failure being widely accepted(Alano et al., 2010; Heeres and Hergenrother, 2007; Virag et al., 2013). Recently, it has been recognized that PAR polymers, the products of PARP-1 activation, are realized to play a prominent role in cell death by triggering the translocation of apoptosis inducing factor (AIF) from mitochondrial to nuclear.(Wang et al., 2009; Yu et al., 2002, 2006). PARP-1-mediated cell death has been reported to occur in several toxic or stressful insults conditions(Ba and Garg, 2011; Gero and Szabo, 2006). In particular, increasing evidence indicates that this type of cell death is involved in many disease models like ischemia, inflammation and diabetes(Fatokun et al., 2014; Gero and Szabo, 2006).

Host cells usually undergo cell death in response to infection of a number of viruses. To directly explore which type of programmed cell death was induced by ZIKV infection, we examined the markers of different types of cell death and analyzed the associated mechanisms. In this study, we demonstrate that PARP-1 mediated cell death is observed in cells infected with ZIKV or over-expressing NS3 protein, and in both cases PARP-1 is significantly activated. Meanwhile, the intracellular ATP and NAD^+ are largely attenuated in ZIKV infected cells, though AIF nuclear translocation was barely detected. Mass spectrometry analysis indicated that NS3 interacted with PARP-1, and PARP-1 was activated by NS3. PARP-1 knockdown or inhibition of PARP-1 activity by pharmaceuticals could suppress the cell death induced by ZIKV. Thus, our finding identifies a novel mechanism of cell death induced by ZIKV which is dependent on PARP-1 activation.

2. Results

2.1. Programmed cell death was induced during ZIKV infection

Previous studies revealed that ZIKV infection caused neuronal death (Gaburro et al., 2018; Ghouzzi et al., 2017; Oh et al., 2017), but the molecular determinants of this cell death remain unclear. To investigate if any specific type of programmed cell death was induced by ZIKV infection, we first established a cell model to support ZIKV infection. Cell death was surveyed by Propidium Iodide (PI) staining and quantified by measuring intracellular ATP. We observed that ZIKV can infect Hela cells effectively as the viral proteins NS1 and NS3 were detected (Fig. 1A). Cell death was detected 48 h post ZIKV infection as indicated by the large attenuation of intracellular ATP and increase in PI positive cells(Fig. 1B). These results suggest that ZIKV infection could induce notable cell death.

Programmed cell death was executed through specific intracellular biochemical pathways. As described above, apoptosis is executed by a group of caspases. Upon caspase activation and subsequent cleavage of intracellular substrates (cleavage of PARP-1 by caspases has been identified as one of the first biochemical markers of apoptosis), cells break into small membrane-wrapped vesicles(Germain et al., 1999). Necroptosis is mediated by RIPK3-MLKL complex and pyroptosis is defined as gasdermin-mediated programmed cell death with caspase1 activation. It is well known that RIPK3 is not expressed in Hela cells, therefore, RIPK3-dependent necrosis is unlikely to contributed to ZIKV-induced cell death. Therefore, we utilized caspase1 cleavage as the marker of Pyroptosis and PARP-1 cleavage as the marker of apoptosis to define the specific type of cell death induced by ZIKV. Hela cells were infected with 1 MOI ZIKV for the indicated time and cells extracts were subjected to western blot analysis. Of note, we did not observe caspapse1 cleavage but strong PARP-1 cleavage, which suggested that pyroptosis was not involved in ZIKV infection-induced cells death (Figs. 1C and S1). Taken together, the above findings indicated that ZIKV infection specifically induced cell apoptosis instead of necrosis or pyroptosis.

The ZIKV genome can be directly translated into a single polyprotein which can be cleaved by viral and host proteases into structural proteins and nonstructural proteins (NS)(Li et al., 2017). To dissect which proteins from ZIKV were responsible for the cell death, 5 nonstructural proteins were transfected into HEK-293T cells and cell death was studied by measuring PARP-1 cleavage. Intriguingly, significant PARP-1 cleavage was detected in NS3 transfected cells but not in NS1, NS4A, NS4B and NS5 transfected cells (Fig. 1D). These results suggest that ZIKV NS3 protein is the dominant inducer of cell death during ZIKV infection. To further confirm the cytotoxicity of NS3,both PI staining and the ATP assay were applied. HEK-293T cells were transfected with HA-NS3, HA-NS5 or HA-vector for 48 h, cells were stained with PI or lysed to measure ATP. Compared to the empty vector or NS5 transfected cells, the viability of the NS3 overexpressing cells was much lower and more PI positive cells were detected in NS3 transfected cells (Fig. 1E).

Collectively, these findings demonstrate that ZIKV infection triggers apoptosis in Hela cells and the viral helicase NS3 is the inducer.

2.2. Dissecting the underlying death signaling triggered by NS3

To explore how ZIKV NS3 induced cell death, we sought to identify the proteins associated with NS3 in host cells. HA-NS3 was transfected into HEK-293T cells and NS3 complex was pulled down by immunoprecipitation with an anti-HA antibody. The precipitate was subjected to SDS/PAGE and stained with coomassie, and analyzed by protein mass spectrometry (Fig. 2A). The analysis revealed that PARP-1 peptides were enriched more in NS3 immunoprecipitation group compared with that of the vector control group (Fig. 2B & Additional file 1: Table 1), which indicated that PARP-1 might be a candidate binding protein for NS3. Transient transfection and co-immunoprecipitation experiments confirmed that PARP-1 can bind to NS3 (Fig. 2C). Furthermore, endogenous PARP- 1 was also found to associate with NS3 but not NS5 (Fig. 2D).

To further determine which domains in NS3 and PARP-1 were responsible for the interaction, a panel of PARP-1 and NS3 truncation variants were constructed. PARP-1 is a 1014 residue protein comprising several well characterized structural or functional domains: 1)a DNA binding domain (DBD, aa 1–372), 2)an auto modification domain (BRCT, aa 372–524), 3) a WGR (Trp–Gly–Arg) motif (aa 525–643), and 4) a catalytic domain (CA, aa 654-1014) (Kraus and Hottiger, 2013). The NS3 protein is composed of a protease domain (aa:1-169), a helicase domain (aa: 179-618) and a 10- residues linker. Domain-mapping experiments indicated that the WGR motif of PARP-1 and protease domain of NS3 were crucial for the interaction between PARP-1 and NS3 (Fig. 2E and F).

2.3. PARP-1 interacts with NS3 during ZIKV infection

To further validate the interaction of PARP-1 and NS3 in vivo, Hela cells were infected with ZIKV for 36 h, and cell extracts were

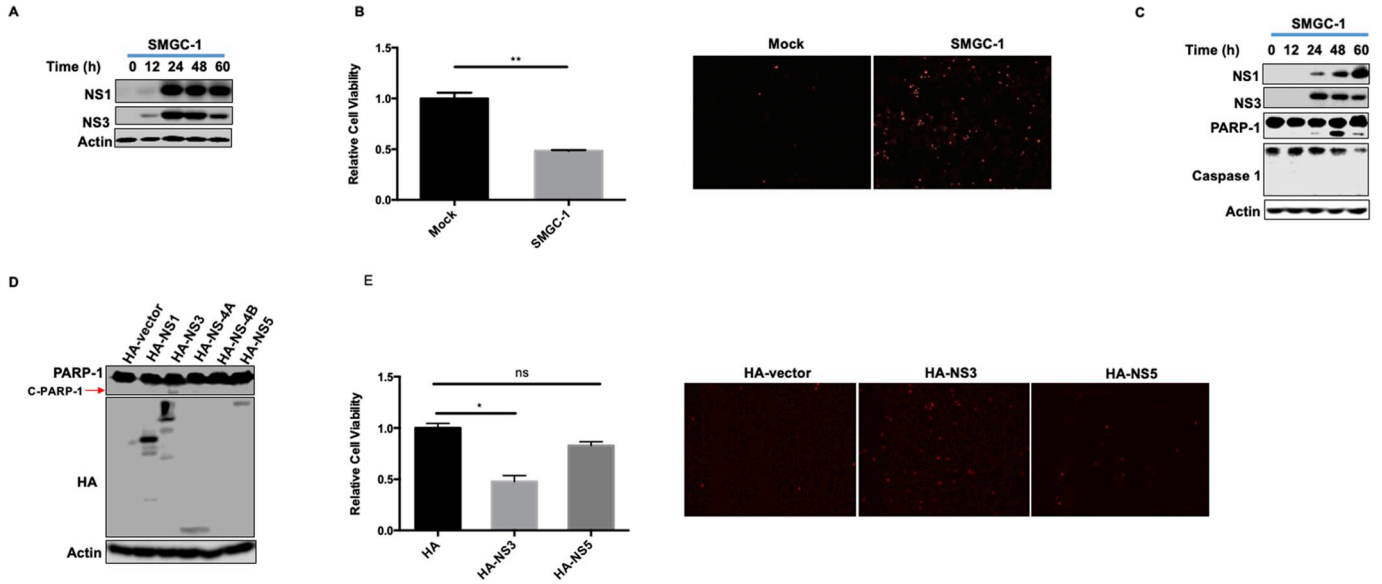

Fig. 1. Programmed cell death was induced during ZIKV infection. (A) Hela cells were infected with SMGC-1 at a MOI of 1 for the indicated time. Viral protein expression was measured by Western-blot analysis. (B) Hela cells were infected with SMGC-1 at a MOI of 1 for 48 h, cell death was analyzed by measuring ATP levels and PI staining. (C) Hela cells were infected with SMGC-1 at a MOI of 1 for indicated time, PARP-1 and caspase1 cleavage were measured by Western-blot analysis. (D) 5 nonstructural proteins and vector control were transfected into HEK-293T cells for 48 h. cell lysates were subjected to Western-blot analysis. (E) NS3, NS5 and vector plasmids were transfected into HEK-293T cells for 48 h and the extent of cell death was analyzed by measuring ATP levels and PI staining.

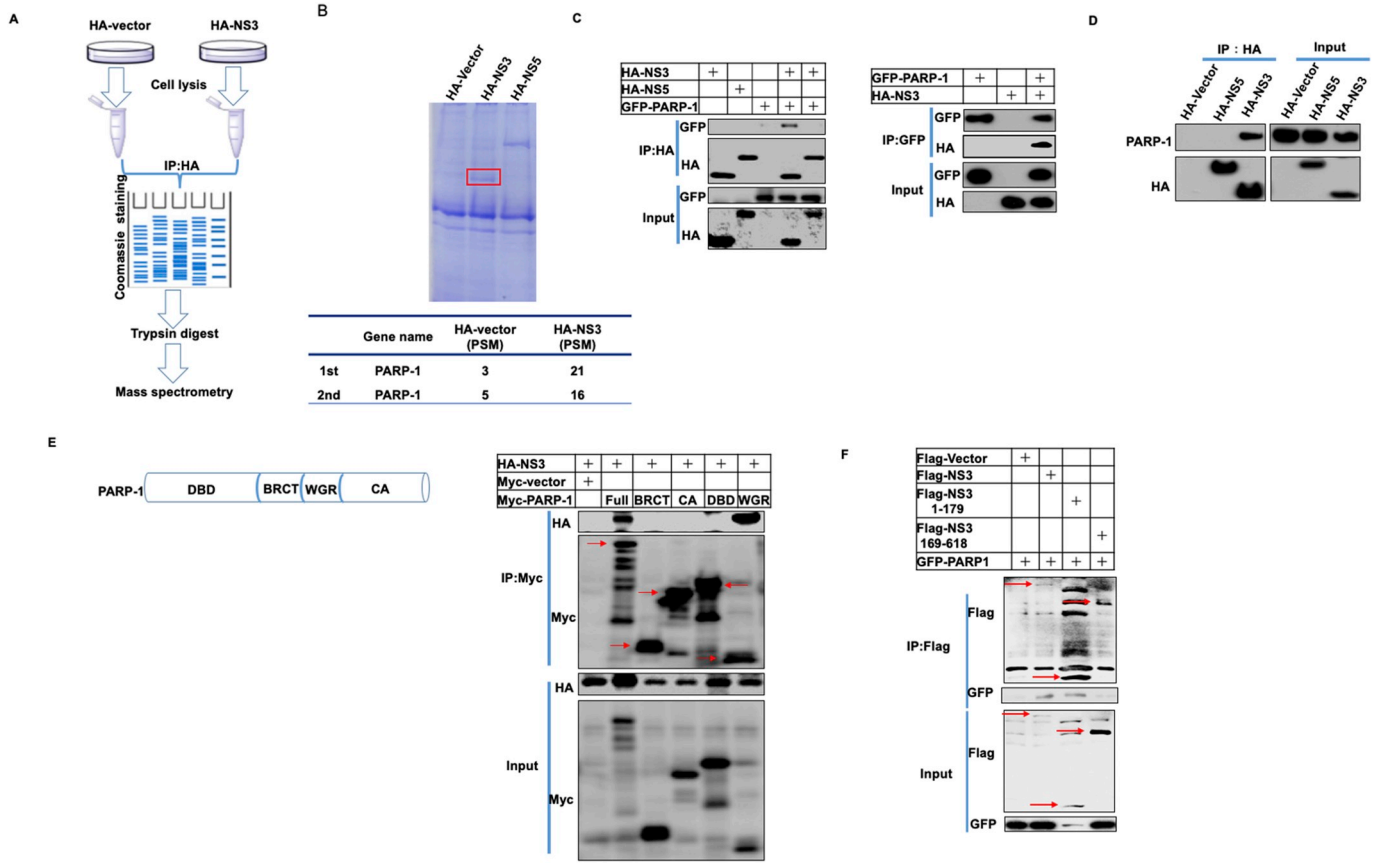

Fig. 2. Dissecting the underlying death signaling triggered by NS3. (A) Schematic of the mass spectrometry analysis of NS3 immunocomplex. (B) The precipitate was subjected to SDS/PAGE and stained with Coomassie. The numbers of PARP-1 peptides detected by MS were shown in two separate experiments. (C) HEK293T cells were transfected with the indicated plasmids for 24 h before co-immunoprecipitation and immunoblot analysis with the indicated antibodies. (D) HEK-293T cells were transfected with HA-vector, HA-NS3 or HA-NS5 for 48 h. Then the cell lysates were immunoprecipitated with anti-HA and the immunocomplex was analyzed by Western-blot. (E) HEK293T cells were transfected with plasmids expressing various truncated PARP-1 proteins, followed by immunoprecipitation and Western blotting. Schematic representations are also shown. (F) NS3 truncation expression constructs were co-transfected with GFP-PARP-1, followed by immunoprecipitation and Western blotting.

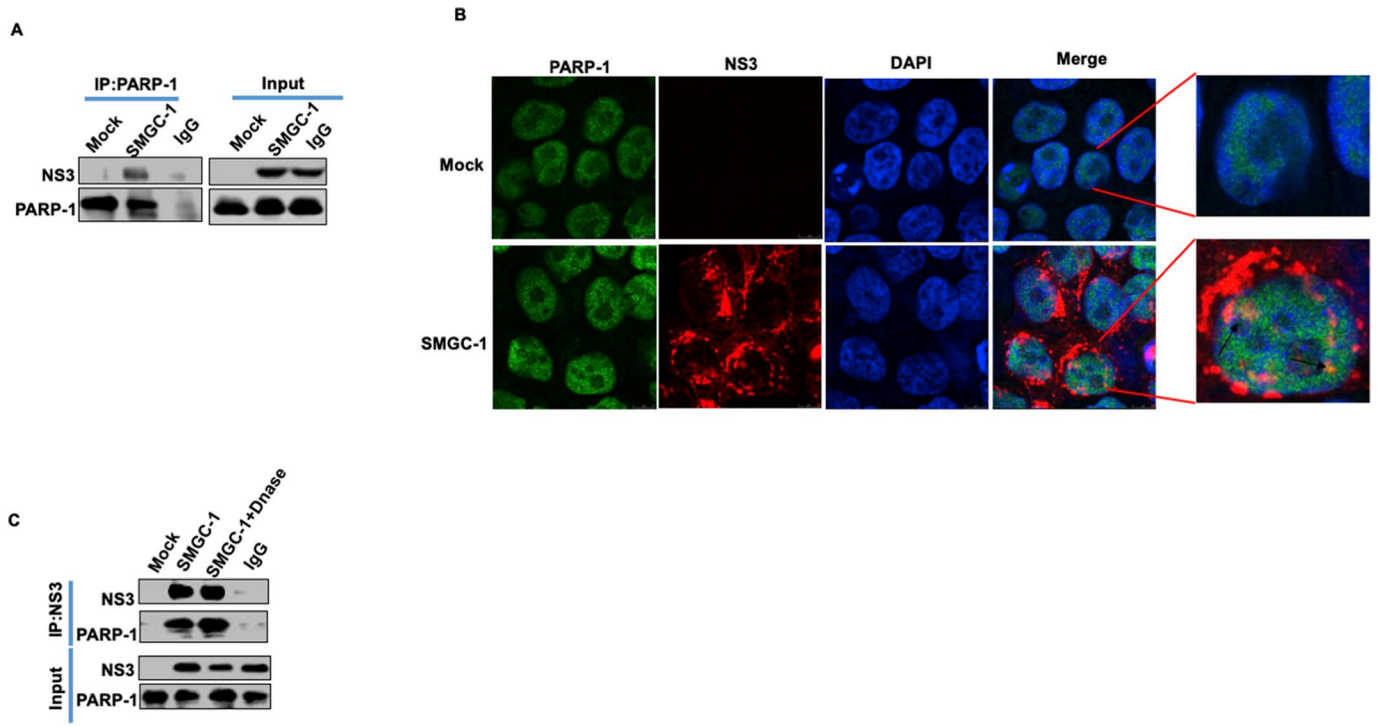

Fig. 3. PARP-1 interacts with NS3 during ZIKV infection. (A) Hela cells were infected with 1MOI SMGC-1 for 48 h. Endogenous co-immunoprecipitation and immunoblotting analysis were performed with the indicated antibodies. (B) Hela cells were infected with 1MOI SMGC-1 for 48 h, PARP-1 and NS3 co-localization was analyzed by Confocal microscopy. (C) Hela cells were infected with 1MOI SMGC-1 for 48 h, cell lysates were treated with DNase and then immunoprecipitated with anti-NS3, the interaction of PARP-1 and NS3 was examined by Western blotting.

immunoprecipitated with an anti-PARP-1 antibody. Consistent with the above findings, PARP-1 was found to bind to NS3 during ZIKV infection (Fig. 3A). Furthermore, NS3 was co-localized with PARP-1 in ZIKV infected cells detected by immunofluorescence analysis (Figs. 3B and S3). To rule out the non-specific interaction between NS3 and PARP-1, which is mediated through simultaneous binding to nucleic acids, DNase was added into the cell extract before the immunoprecipitation. NS3 still bound to PARP-1 in the presence of DNase (Fig. 3C). Collectively, these finding suggest that PARP-1 might partner with NS3 and participate in ZIKV infection-induced cell death.

2.4. PARP-1 activation correlated with the cell death during ZIKV infection

Having demonstrated that NS3 interact with PARP-1, we hypothesized that the interaction might trigger cell death through activation of PARP-1. To assess the possibility, Hela cells were infected with 1 MOI ZIKV for the indicated time point. PARP-1 activation, represented by the levels of PAR polymers. and cell death, represented by PARP-1 cleavage, were evaluated by Western blotting. Indeed, we discovered that the levels of PAR polymers were greatly increased after ZIKV infection (Fig. 4A). PARP-1 activation and cell death were also detected in nerve cell SF268 after ZIKV infection (Fig. S2). These findings suggested that the cell death induced by the ZIKV infection might be a result of the PARP-1 activation. In addition to PARP-1, other PARPs can also catalyze PAR production. To determine whether the PAR was synthesized specifically by PARP-1, we generated PARP-1 knock down (KD) cells by Lentivirus and observed that excess PAR was produced in WT cells after ZIKV infection, but much less PAR was synthesized in the PARP-1 KD cells (Fig. 4B). Simultaneously, inhibition of PARP-1 expression in Hela cells attenuated ZIKV-induced cell death, indicated by better viability and less PI staining was detected in PARP-1 deficient cells (Fig. 4C).

It has been reported that excessive PARP-1 activation leads to cell death due to energy exhaustion or AIF translocation (Alano et al., 2010; Yu et al., 2006). Therefore, we next examined the nuclear translocation of AIF in mock and ZIKV infected cells. Very little nuclear translocation of AIF was detected in ZIKV infected cells and most AIF was residing in mitochondria (Fig. 4D). The cell death characterized by PARP-1 activation without the AIF nuclear translocation was also reported in others' studies(Erdelyi et al., 2009; Robaszkiewicz et al., 2012). Therefore, we next evaluated the level of NAD^+ in the cells after viral infection and observed that intracellular NAD^+ was significantly reduced after viral infection, but knock-down PARP-1 can rescue NAD^+ decline (Fig. 4E). These results indicated that the PARP-1-mediated cell death induced by ZIKV infection was due to intracellular energy failure but not to AIF nuclear translocation.

To further explore whether ZIKV NS3 directly activated PARP-1, we transfected HA-NS3 and vector control into HEK-293T cells and found PAR was accumulated in NS3 over-expressing cells but dropped rapidly when the PARP-1 inhibitor Olaparib was added (Fig. 4F), which suggested that the PAR accumulation induced by NS3 was dependent on PARP-1. Taken together, our findings provide strong evidence that ZIKV infection induces excessive PARP-1 activation, PAR accumulation and ultimately gives rise to cell death and this is most likely dependent on ZIKV protein NS3.

2.5. The activity of PARP-1 was unnecessary for the NS3-PARP-1 interaction but essential for cell death

To further address the importance of PARP-1 activation in ZIKV-induced cell death, the PARP-1 inhibitor Olapairb was added during ZIKV infection. We evaluated the extent of cell death by PI staining and ATP assay in ZIKV infected cells with or without Olapairb treatment. Consistent with the above findings, ZIKV infection induced cell death, and the PARP-1 inhibitor could block the cell death greatly (Figs. 5A and S1). Consistently, both PARP-1 cleavage and PAR production were suppressed in Olapairb treated cells (Fig. 5B). Thus, these results indicate that the activity of PARP-1 was necessary for the cell death induced by ZIKV.

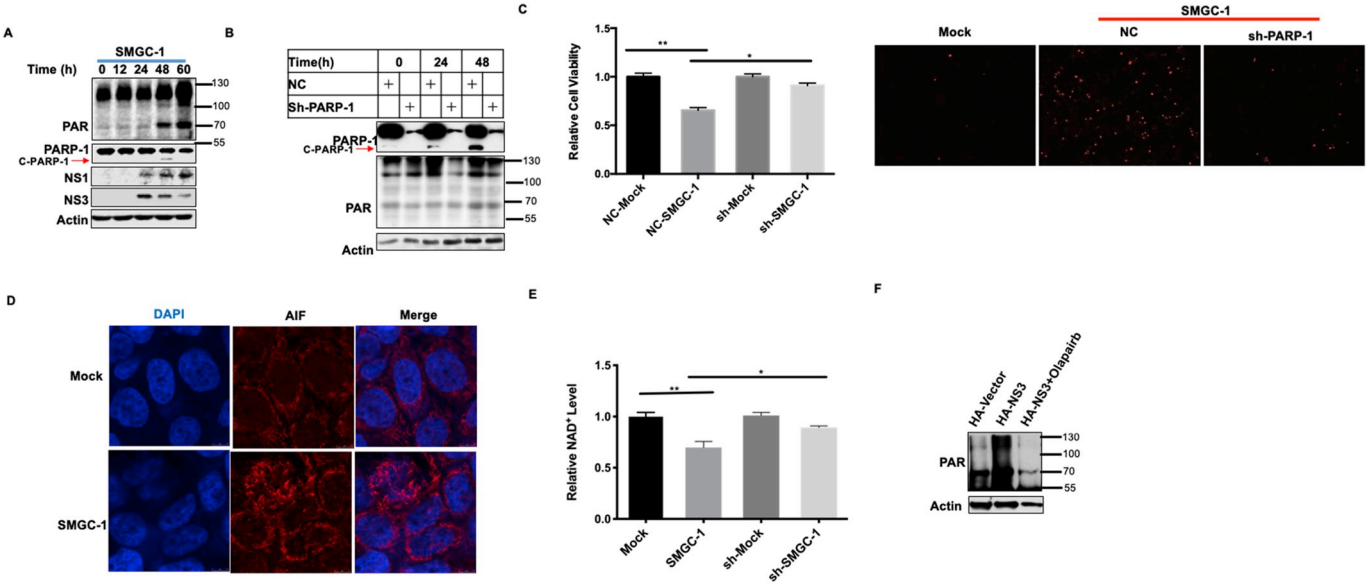

Fig. 4. PARP-1 activation correlated with the cell death during ZIKV infection. (A) Hela cells were infected with 1MOI SMGC-1 for the indicated time. Cell lysates were then collected and subjected to Western-blot analysis using the indicated antibodies. (B) PARP-1 WT/KD Hela cells were infected with SMGC-1 at 1MOI for 24 and 48 h. Cells were harvested and lysed to Western-blot analysis with the indicated antibodies. (C) PARP-1 WT/KD Hela cells were infected with SMGC-1 at 1MOI for 48 h, cell death was analyzed by measuring ATP levels and PI staining. (D) Confocal microscopy analysis of AIF localization in Hela cells with or without ZIKV infection for 48 h. (E) PARP-1 WT/KD Hela cells were infected with 1MOI SMGC-1 for 48 h, the NAD^+ level was determined by NAD/NADH-GloTM Assay. (F) NS3 transfected HEK-293T cells incubated with DMSO or 5 μM PARP-1 inhibitor Olapairb for 12 h, the cells were harvested for Western-blot.

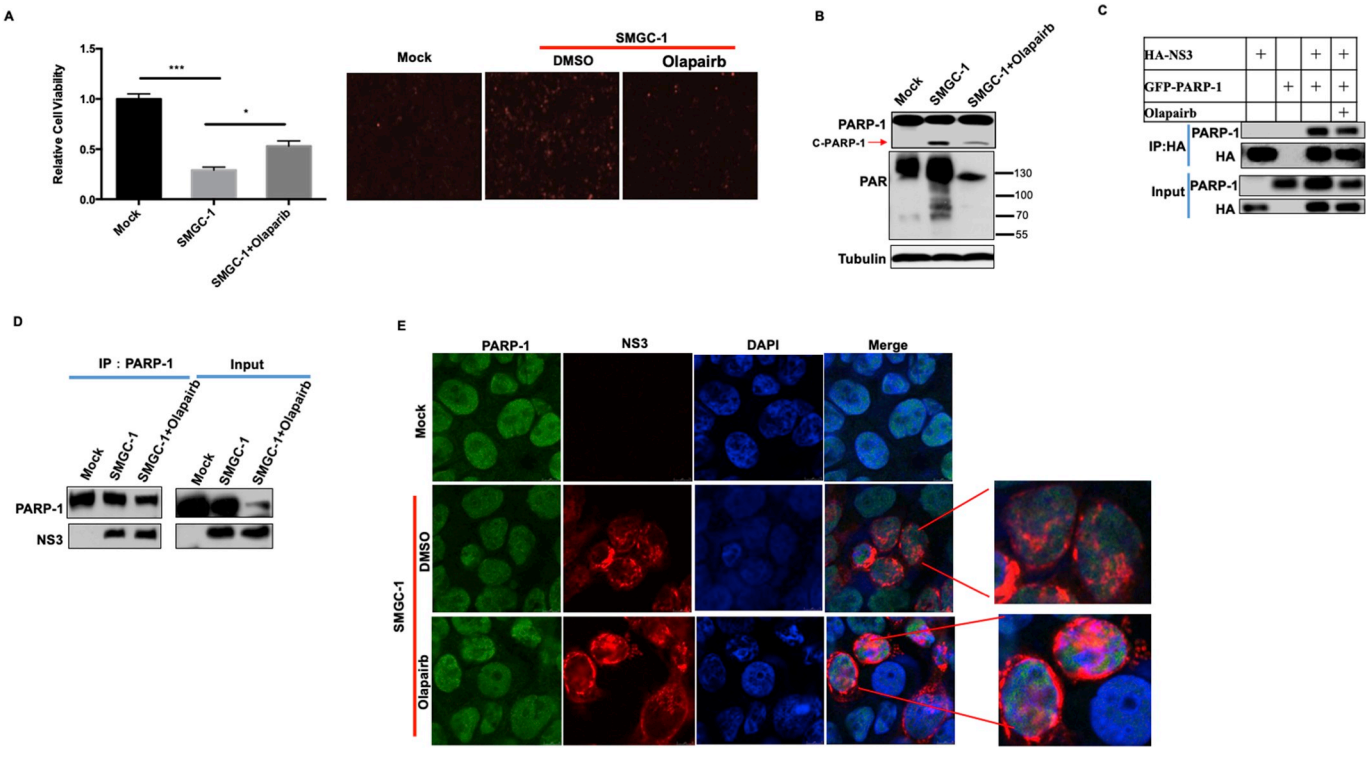

Fig. 5. The activity of PARP-1 was unnecessary for the NS3-PARP-1 interaction but essential for cell death. (A)Hela cells were infected with 1MOI SMGC-1 for 24 h, then 5uM Olapairb were added for 24 h. Cell death was examined by PI staining and measuring ATP levels. (B) 24 h after infection with ZIKV, cells were incubated with 5uM Olapairb for 24 h. Cell lysates were analyzed by western blotting with the indicated antibody. (C) HEK293T cells were transfected with the indicated plasmids for 24 h and then treated with 5um Olapairb for 24 h before co-immunoprecipitation and immunoblot analysis with the indicated antibodies. (D) 24 h after infection with ZIKV, Hela cells were incubated with 5uM Olapairb for 24 h. Cell were harvested and lysed to immunoprecipitate with anti-PARP-1 antibody. (E) 24 h after ZIKV infection, Hela cells were treated with 5uM Olapairb for 24 h. PARP-1 and NS3 co-localization was analyzed by Confocal microscopy.

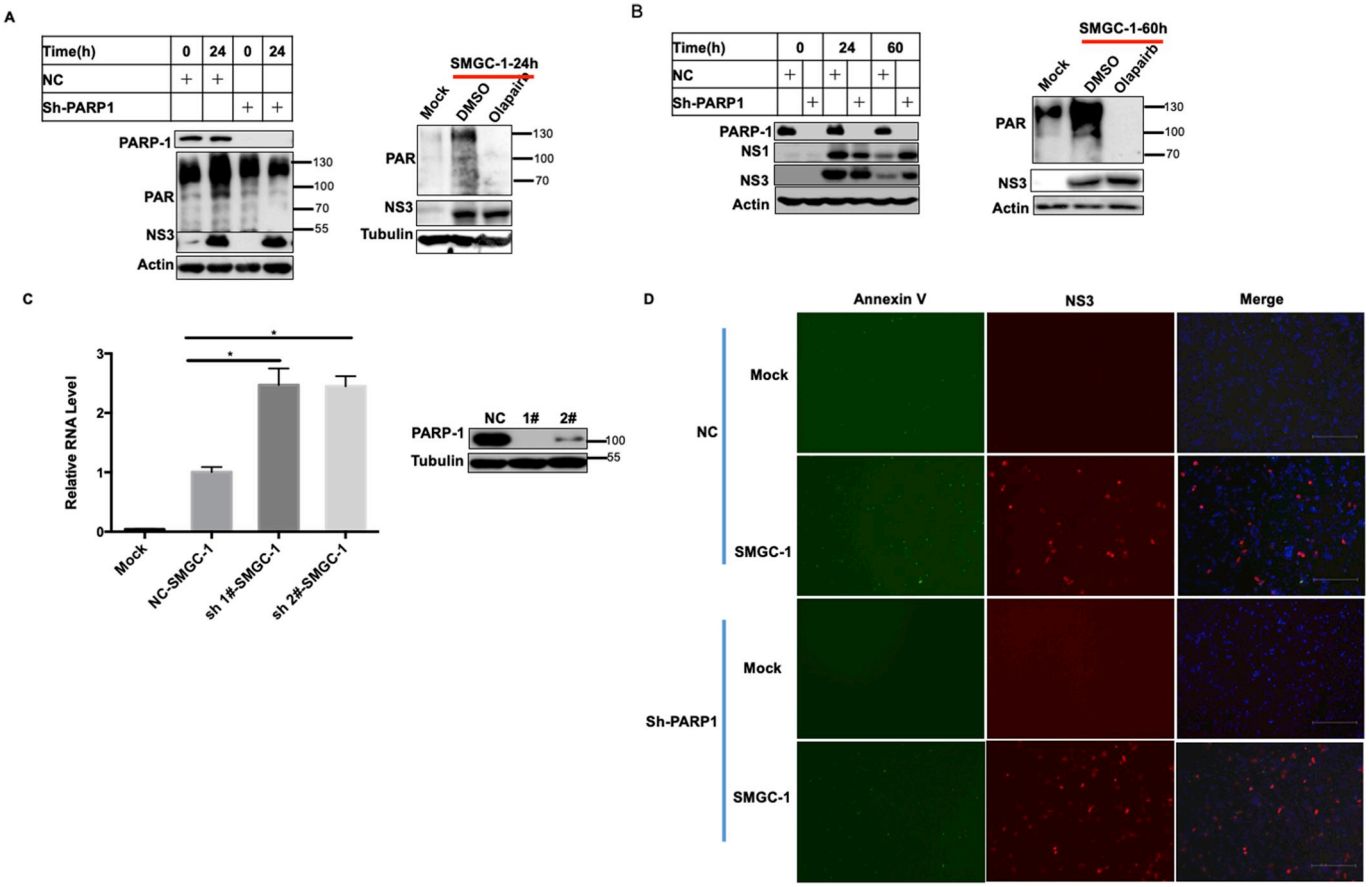

Fig. 6. PARP-1 was dispensable for ZIKV replication but PARP-1 mediated cell death limited virus infection. (A) WT and PARP-1 KD Hela cells were infected with SMGC-1 at 1MOI for 24 h (left), Hela cells were treated with Olapairb for 24 h while infecting the virus(Right),viral protein expression was measured by Western-blot analysis. (B) WT and PARP-1 KD Hela cells were infected SMGC-1 at 1MOI for 24 h and 60 h(left), 24 h after infection with ZIKV, Hela cells were incubated with 5uM Olapairb for 48 h(Right),viral protein expression was measured by Western-blot analysis. (C) WT and PARP-1 KD Hela cells were infected SMGC-1 at 1MOI for 60 h, the intracellular viral RNA was determined by RT-qPCR. Knockdown efficiency of PARP-1in Hela cells was measured by Western blotting. (D) WT and PARP-1 KD Hela cells were infected with SMGC-1 at 1MOI for 60 h, cell death was analyzed by staining with Alex-488 labelled anti-Annexin V first and viral protein expression was measured by staining with anti-NS3.

Next, we explored whether the protective effect of PARP-1 was mediated through blocking the interaction between PARP-1 with NS3. GFP-PARP-1 and HA-NS3 were co-transfected into HEK-293T cells and treated with the PARP-1 inhibitor Olapairb for 12 h, cell extracts were subjected to a co-immunoprecipitation assay. In the presence of inhibitors, PARP-1 can still bind to NS3(Fig. 5C). We also investigated the effect of the PARP-1 inhibitor on the interaction between NS3 and PARP-1 under ZIKV infection. Hela cells were infected with 1 MOI ZIKV for 24 h and then treated with Olaparib for 24 h, the binding of NS3 and PARP-1 was detected by co-immunoprecipitation and immunoblotting analyses. In agreement with the above result, Olaparib cannot disrupt the interaction between NS3 and PARP-1 during ZIKV infection (Fig. 5D). From the perspective of immunofluorescence, the PARP-1 inhibitor Olaparib did not affect the co-localization of NS3 and PARP-1 (Fig. 5E). Thus, the activity of PARP-1 did not affect the interaction of NS3-PARP-1, but was essential for the cell death, indicating that the interaction of NS3 and PARP-1 was not enough to induce cell death and thus that PARP-1 activation is the key to inducing cell death.

2.6. PARP-1 was dispensable for ZIKV replication but PARP-1 mediated cell death limited virus infection

To investigate how the loss or inactivation of PARP-1 affects ZIKV replication, PARP-1 WT/KD Hela cells or DMSO/Olapairb treated Hela cells were infected with 1MOI ZIKV for 24 h and cell extracts were applied to Western blot. No significant difference in the levels of the viral protein was observed (Fig. 6A). These data suggest that PARP-1 is dispensable for ZIKV entry and replication.

Persistent cell death could limit virus infection by eliminating the intracellular niche of virus. Therefore, we investigated the consequence of PARP-1 mediated cell death during ZIKV infection. 1MOI ZIKV was used to infect WT and KD cells for 24 h and 60 h, the levels of viral proteins were examined by Western blot. WT Hela cells died after infection of ZIKV for 60 h, leading to reduced expression of virus proteins compared to that observed in PARP-1 KD cells (Fig. 6B). Hela cells were treated with PARP-1 inhibitor for 48 h after virus infection for 24 h, which also partially inhibited virus replication (Fig. 6B). We also detected the intracellular viral RNA in PARP-1 WT/KD cells 60 h post infection with ZIKV. Consistently, more intracellular viral RNA was detected in PARP-1 KD cells (Fig. 6C). The results of immunofluorescence also confirmed that PARP-1-mediated cell death contributes to limiting virus infection (Fig. 6D).

Collectively, our findings demonstrate that ZIKV can activate PARP-1 mediated cell death and the cell death feedback to suppress viral replication even if PARP-1 is dispensable for ZIKV replication.

3. Discussion

ZIKV infection has emerged as a global health threat(Haug et al., 2016). Therefore, investigation into the virus including its pathogenicity, the clinical symptoms and the interaction with host are particularly important. In our study, we uncovered a novel mechanism of

programmed cell death induced by ZIKV which functioned critically for host defenses against ZIKV. This cell death is initiated by the interaction of the ZIKV helicase NS3 with PARP-1 and executed by excessive PARP-1 activation.

Cell death induced by ZIKV has been reported in several studies: in mice models, ZIKV infection induced cell death mainly in neurons and the increase in cell death contributed to the smaller size of infected brains(Ghouzzi et al., 2016). In addition, significantly higher caspase-3 activation in hNPCs 3 days after ZIKV infection was discovered(Oh et al., 2017). P53 activation and genotoxic stress elicited by ZIKV infection were also detected in hNPCs infected with ZIKV(Ghouzzi et al., 2017). Collectively, the findings from these studies prove that ZIKV infection could induce cell death. But many questions were unanswered: first, which type of PCD was induced by ZIKV infection? Second, whether a specific element of ZIKV was responsible for the cell death? And finally, what was the effect of cell death on ZIKV infection? To address these questions, we generated a cell model which not only supported ZIKV infection but also was easy to examine the resulting cell death. In our study, we found that cell death can be effectively induced during ZIKV infection and NS3 was identified as the major factor.

NS3 was found to be crucial for both viral polypeptide processing and genomic replication, mediated through its N-terminal protease domain and a C-terminal helicase domain, respectively. NS3 facilitated virus replication by providing chemical energy to unwind viral RNA replication intermediates(Saw et al., 2017), making NS3 a preferred choice for drug development(Chan et al., 2017; Yuan et al., 2016). Although it was important, less was known about the interaction between NS3 and host proteins compared to other ZIKV proteins. Here, we report a previously uncharacterized interaction between ZIKV NS3 with the host protein PARP-1. PARP-1 was shown by mass spectrometry and co-immunoprecipitation to interact with NS3 by mass spectrometry and confirmed by co-immunoprecipitation. What surprised us was that a part of NS3 could enter into the nucleus and co-localize with PARP-1.

PARP-1, a Poly(ADP-ribose) polymerase which transferred negatively charged ADP-ribose units from donor NAD^+ onto various substrates such as mono or poly (ADP-ribose) chains played diverse roles in multiple cellular processes (Bouchard et al., 2003; Meder et al., 2005). Recent studies reported a cell death mediated by the over activation of PARP-1. The excessive activation of PARP-1 caused by severe stress resulted in unregulated PAR synthesis and widespread cell death. Energy failure and AIF translocation now are the two well-known mechanisms(Andrabi et al., 2006; Koh et al., 2005; Wang et al., 2016). In the PARP-1-mediated cell death model, caspase was independent but still activated (Wang et al., 2016). So, in our study PARP-1 was cleaved in ZIKV infected cells. We observed that PARP-1 interacted with NS3 through the WGR motif which was reported to be crucial for PARP-1 activation(Li et al., 2014). PARP-1 was activated in ZIKV infected cells resulting in cell death. Cell death and PAR polymer accumulation could be both rescued by knock-down of PARP-1 or addition of PARP-1 inhibitor.

The interaction between virus and host is a long-term process of mutual antagonism: the virus needs to establish a persistent infection to support its replication while the host attempts to eliminate the virus by various modes of immune responses. Pattern recognition receptors (PRRs) are encoded in host cells to monitor virus by activating cytokine expression and engaging cell death signaling(Chow et al., 2015). According to the established model, cell death is considered harmful for the host organism, but PCD is being increasingly appreciated to be beneficial for hosts as it plays an important role in eliminating the intracellular niche of certain pathogens. In our study, we observed that depletion or inactivation of PARP-1 reduces the cell death, but also facilitates virus replication. In this process, the interaction between NS3 with PARP-1 was the prerequisite for PCD, mediated through the activation of PARP-1. It was noteworthy that ZIKV infection or NS3 transfection could trigger PARP-1 activation. We have demonstrated that NS3 binds to PARP-1, but further studies will be required to address how NS3 activates PARP-1. In summary, these findings revealed a new mechanism of cell death induced by ZIKV.

4. Materials and methods

4.1. Cells culture and virus stocks

HEK-293T, Hela cells and SF268 cells (ATCC) were cultured in DMEM containing 10% fetal bovine serum (FBS) and 100 units/ml penicillin/streptomycin. Vero cells (ATCC) were maintained in MEM supplemented with 10% FBS. ZIKV virus SMGC-1(GenBank accession number KX266255) was kindly provided by George Fu Gao (Institute of Microbiology, Chinese Academy of Sciences, Beijing, China), propagated in Vero cells. The virus stocks were titrated in Vero cells by standard plaque-forming assays.

4.2. Antibodies and reagents

Primary antibodies GFP (HT801), HA (HT301), Tubulin (HC101), Actin (HC201) and secondary antibodies Goat Anti-Rabbit (HS101), Goat Anti-Mouse (HS201) were purchased from TransGen Biotech. Anti-PAR Rabbit Polyclonal Antibody (Catalog #: 4336-BPC-100) was from Trevigen. PARP (46D11) Rabbit mAb (#9532), HA-Tag (C29F4) Rabbit mAb (#3724) used for western blot were purchased from Cell Signaling. PARP1 Mouse Monoclonal antibody (66520-1-Ig) used for immunoprecipitation was from Proteintech. Mouse Anti-Cleaved PARP (552597) was used for Immunofluorescence microscopy from BD Biosciences. Rabbit polyclonal anti-NS3 and anti-NS1 were kindly provided by George Fu Gao. PARP-1 inhibitor Olaparib (CAS number: 763113-22-0) was purchased from Selleck.

4.3. Plasmid and transfection

ZIKV NS3 gene was generated by PCR amplification from the cDNA of ZIKV infected Vero cells. The primers: Forward: 5′-*ATGAAAAGGAG TGGTGCTCTATGG-3′*, reverse: 5′-*CCCGCGGCAACTCTT*-3′ were used to amplify full length NS3 which was cloned into the pcDNA3.1-HA vector. GFP-PARP-1 was kindly provided by Xueqing Ba (Northeast Normal University, Changchun, China). Myc-PARP-1 and the series of truncation PARP-1 plasmid were from Bin Li (Institut Pasteur of Shanghai, Chinese Academy of Sciences, Shanghai, China). HEK-293T and Hela cells were transfected using the polyethylenimine (PEI, Polysciences). Briefly, 5×10^5 cells were seeded onto 6-well culture plates and settled for 12 h. 3ug plasmid was diluted in 50ul opti-DMEM, 6ul (1 mg/ml) PEI was added and vortexed immediately. The mixture was incubated at room temperature for 10min and then added to cells. After 48 h, cells can be harvested for Western blot or co-immunoprecipitation assay.

4.4. Generation of PARP-1-shRNA cells

Two PARP-1 shRNA: (1# shRNA : 5′-*CCGGCGACCTGATCTGGAAC ATCAACTCGAGTTGATGTTCCAGATCAGGTCGTTTTTG-3′* and 2# shRNA2 : 5′-*CCGGCTTCGTTAGAATGTCTGCCTTCTCGAGAAGGCAGAC ATTCTAACGAAGTTTTTG-3′*) were cloned into PLKO.1 vector. 2 μg plasmids including the expression vector and the packaging plasmids were transfected into HEK-293T cells in 6-well plates for 48 h and the media containing the virus were collected and filtered through a 0.45-μM PVDF membrane (Millipore). Transduction was performed by incubating cells with collected Lentivirus in the presence of 8 μg/ml Polybrene. 48 h later, 5 μg/ml puromycin were added for 2–3 days to establish stable sh-PARP-1 Hela cells.

4.5. Western blot

Transfected cells or virus infected cells were harvested, washed by

PBS and lysed with 0.5% NP-40 buffer supplemented with protein inhibitor cocktail, NaVO3 and NaF for 40 min at 4 °C. The supernatants were collected by centrifugation for 15 min at 4 °C and protein concentrations are analyzed by BCA assay kit (Thermo). Equal amounts of proteins were separated by 9% SDS-PAGE and electrophoretically transferred onto a 0.22μm NC membrane. After blocking with 5% non-fat milk in TBST, the membranes were incubated with the primary antibodies overnight at 4 °C. After washing 3 times with TBST, membranes were incubated with HRP labelled secondary antibody at room temperature for 1 h.

4.6. Co-immunoprecipitation and immunoblotting analysis

ZIKV infected Hela cells or HEK-293T cells Transfected with indicated plasmids were harvested, washed with PBS and lysed in in 0.5% NP-40 buffer containing protein inhibitor cocktail, NaVO3 and NaF. Supernatants were collected via centrifugation and the protein concentrations were analyzed by BCA assay kit. The supernatants were incubated with specific primary antibodies overnight at 4 °C with rotation. 20ul Protein G agaroses was added and incubated at 4 °C for 4 h with rotation. The beads were collected via centrifugation at 5000 rpm for 1 min at 4 °C and washed three times with 1 mL lysis buffer. Then,20μl 2X loading buffer were added and boiled at 100 °C for 5 min. The samples were prepared for western blot.

4.7. Confocal microscopy

Hela cells infected with 1MOI ZIKV virus for 48 h were washed one time with cold PBS and fixed with ice-cold 4% paraformaldehyde (PFA) for 20 min at room temperature. After washing 3 times with PBS, cells were incubated with 0.1% Triton X-100 for 10min. Then the samples were blocked for 1 h using 5% bovine serum albumin. PARP-1(BD,1:500), NS3(1:1000), AIF(PTG,1:500) were used as the primary antibodies incubated overnight at 4 °C or 2 h at room temperature. Fluorescently labelled secondary antibodies (1:500) were diluted in 2% BSA and incubated for 1 h at room temperature and then stained with DAPI. The samples were observed with LEICA SP8 confocal microscope under a 63X water objective.

4.8. PI staining

HEK-293T cells transfected with HA-NS3, HA-NS5 or vector for 48 h or Hela cells infected 1MOI ZIKV for 48 h were stained with 1 mg/ml Propidium iodide (CAS: 25535-16-4, Sangon Biotech) then evaluated by fluorescence microscopy (Olympus).

4.9. RT-PCR and qPCR

Total RNA was extracted with TRIzol Reagent (Invitrogen) in accordance with the manufacturer's instructions and reverse-transcribed into cDNA with a High-Capacity cDNA Reverse Transcription Kit (Applied Biosystems). The expression levels of viral RNA were determined by qPCR analysis using Power SYBR Green PCR Master Mix (Applied Biosystems). The real-time PCR primers set for ZIKV RNA detection were as follows: forward (5′-*TGAYAAGCARTCAGACAC*-3′) and reverse (5′-*TCACCARRCTCCCTTTGC*-3′).

4.10. Measurement of intracellular NAD + and ATP levels

The cellular ATP content of the lysates was determined using CellTiter-Glo Luminescent Cell Viability Assay (Promega, USA), following the manufacturer's instruction. Total NAD and NADH were determined with NAD/NADH quantification kit NAD/NADH-GloTM Assay (Promega, USA).

4.11. Statistics

All statistical analyses are performed using GraphPad Prism software. Data were derived from the average of three biological replicate experiments, and calculated as the mean ± SEM. The difference was analyzed by the Student's t-test. *, $P < 0.05$, **, $P < 0.01$.

Author contributions

G.X designed the experiments and wrote the draft of the manuscript. S-. H. L, X-. Y. L Y.Y and P.G, helped perform the experiments and contributed to data analysis. X-.T.C and H-. Y. W contributed to the writing. M-. X. Z and F.G contributed to data analysis and coordinated the project. F–P. Z provided ideals and revised the manuscript.

Financial support

This work was supported by grants from Jin Qi team of Sanming Project of Medicine in Shenzhen (SZSM201412001) and the National Key Research and Development Project (2016YFC1200302).

Conflict of interest

The authors declare that they have no conflict of interest.

Acknowledgements

We thank professor George Fu Gao at Institute of Microbiology, Chinese Academy of Sciences, Beijing, China for providing Zika virus SMGC-1 and ZIKV NS3 rabbit polyclone antibody and his help in the propagation of Zika virus. We thank professor Xueqing Ba (Northeast Normal University, Changchun, China) for providing GFP-PARP-1 plasmid. We also thank professor Bin Li (Institute Pasteur of Shanghai, Chinese Academy of Sciences, Shanghai, China) for providing Myc-PARP-1 and the series of truncation PARP-1 plasmids.

Appendix A. Supplementary data

Supplementary data to this article can be found online at https://doi.org/10.1016/j.virol.2019.08.024.

References

Alano, C.C., Garnier, P., Ying, W., Higashi, Y., Kauppinen, T.M., Swanson, R.A., 2010. NAD + depletion is necessary and sufficient for poly(ADP-ribose) polymerase-1-mediated neuronal death. J. Neurosci. 30, 2967–2978.

Andrabi, S.A., Kim, N.S., Yu, S.W., Wang, H., Koh, D.W., Sasaki, M., Klaus, J.A., Otsuka, T., Zhang, Z., Koehler, R.C., Hurn, P.D., Poirier, G.G., Dawson, V.L., Dawson, T.M., 2006. Poly(ADP-ribose) (PAR) polymer is a death signal. Proc. Natl. Acad. Sci. U. S. A. 103, 18308–18313.

Ba, X., Garg, N.J., 2011. Signaling mechanism of poly(ADP-ribose) polymerase-1 (PARP-1) in inflammatory diseases. Am. J. Pathol. 178, 946–955.

Bouchard, V.J., Rouleau, M., Poirier, G.G., 2003. PARP-1, a determinant of cell survival in response to DNA damage. Exp. Hematol. 31, 446–454.

Chambers, T.J., Hahn, C.S., Galler, R., Rice, C.M., 1990. Flavivirus genome organization, expression, and replication. Annu. Rev. Microbiol. 44, 649–688.

Chan, J.F., Chik, K.K., Yuan, S., Yip, C.C., Zhu, Z., Tee, K.M., Tsang, J.O., Chan, C.C., Poon, V.K., Lu, G., Zhang, A.J., Lai, K.K., Chan, K.H., Kao, R.Y., Yuen, K.Y., 2017. Novel antiviral activity and mechanism of bromocriptine as a Zika virus NS2B-NS3 protease inhibitor. Antivir. Res. 141, 29–37.

Chow, J., Franz, K.M., Kagan, J.C., 2015. PRRs are watching you: localization of innate sensing and signaling regulators. Virology 479–480, 104–109.

Dick, G.W., Kitchen, S.F., Haddow, A.J., 1952. Zika virus. I. Isolations and serological specificity. Trans. R. Soc. Trop. Med. Hyg. 46, 509–520.

Erdelyi, K., Bai, P., Kovacs, I., Szabo, E., Mocsar, G., Kakuk, A., Szabo, C., Gergely, P., Virag, L., 2009. Dual role of poly(ADP-ribose) glycohydrolase in the regulation of cell death in oxidatively stressed A549 cells. FASEB J. 23, 3553–3563.

Fatokun, A.A., Dawson, V.L., Dawson, T.M., 2014. Parthanatos: mitochondrial-linked mechanisms and therapeutic opportunities. Br. J. Pharmacol. 171, 2000–2016.

Gaburro, J., Bhatti, A., Sundaramoorthy, V., Dearnley, M., Green, D., Nahavandi, S., Paradkar, P.N., Duchemin, J.B., 2018. Zika virus-induced hyper excitation precedes death of mouse primary neuron. Virol. J. 15, 79.

Galluzzi, L., Kepp, O., Krautwald, S., Kroemer, G., Linkermann, A., 2014. Molecular mechanisms of regulated necrosis. Semin. Cell Dev. Biol. 35, 24–32.
Germain, M., Affar, E.B., D'Amours, D., Dixit, V.M., Salvesen, G.S., Poirier, G.G., 1999. Cleavage of automodified poly(ADP-ribose) polymerase during apoptosis. Evidence for involvement of caspase-7. J. Biol. Chem. 274, 28379–28384.
Gero, D., Szabo, C., 2006. Role of the peroxynitrite-poly (ADP-ribose) polymerase pathway in the pathogenesis of liver injury. Curr. Pharmaceut. Des. 12, 2903–2910.
Ghouzzi, V.E., Bianchi, F.T., Molineris, I., Mounce, B.C., Berto, G.E., Rak, M., Lebon, S., Aubry, L., Tocco, C., Gai, M., Chiotto, A.M., Sgro, F., Pallavicini, G., Simon-Loriere, E., Passemard, S., Vignuzzi, M., Gressens, P., Di Cunto, F., 2016. ZIKA virus elicits P53 activation and genotoxic stress in human neural progenitors similar to mutations involved in severe forms of genetic microcephaly. Cell Death Dis. 7, e2440.
Ghouzzi, V.E., Bianchi, F.T., Molineris, I., Mounce, B.C., Berto, G.E., Rak, M., Lebon, S., Aubry, L., Tocco, C., Gai, M., Chiotto, A.M., Sgro, F., Pallavicini, G., Simon-Loriere, E., Passemard, S., Vignuzzi, M., Gressens, P., Di Cunto, F., 2017. ZIKA virus elicits P53 activation and genotoxic stress in human neural progenitors similar to mutations involved in severe forms of genetic microcephaly and p53. Cell Death Dis. 8, e2567.
Häcker, G., 2018 Oct - Nov. Apoptosis in infection. Microbes Infect. 20 (9–10), 552–559.
Haug, C.J., Kieny, M.P., Murgue, B., 2016. The Zika challenge. N. Engl. J. Med. 374, 1801–1803.
Heeres, J.T., Hergenrother, P.J., 2007. Poly(ADP-ribose) makes a date with death. Curr. Opin. Chem. Biol. 11, 644–653.
Kim, M.Y., Zhang, T., Kraus, W.L., 2005. Poly(ADP-ribosyl)ation by PARP-1: 'PAR-laying' NAD+ into a nuclear signal. Genes Dev. 19, 1951–1967.
Koh, D.W., Dawson, T.M., Dawson, V.L., 2005. Mediation of cell death by poly(ADP-ribose) polymerase-1. Pharmacol. Res. 52, 5–14.
Kraus, W.L., Hottiger, M.O., 2013. PARP-1 and gene regulation: progress and puzzles. Mol. Asp. Med. 34, 1109–1123.
Li, G., Poulsen, M., Fenyvuesvolgyi, C., Yashiroda, Y., Yoshida, M., Simard, J.M., Gallo, R.C., Zhao, R.Y., 2017. Characterization of cytopathic factors through genome-wide analysis of the Zika viral proteins in fission yeast. Proc. Natl. Acad. Sci. U. S. A. 114, E376–E385.
Li, X., Erden, O., Li, L., Ye, Q., Wilson, A., Du, W., 2014. Binding to WGR domain by salidroside activates PARP1 and protects hematopoietic stem cells from oxidative stress. Antioxidants Redox Signal. 20, 1853–1865.
Meder, V.S., Boeglin, M., de Murcia, G., Schreiber, V., 2005. PARP-1 and PARP-2 interact with nucleophosmin/B23 and accumulate in transcriptionally active nucleoli. J. Cell Sci. 118, 211–222.
Mottin, M., Braga, R.C., da Silva, R.A., Silva, J., Perryman, A.L., Ekins, S., Andrade, C.H., 2017. Molecular dynamics simulations of Zika virus NS3 helicase: insights into RNA binding site activity. Biochem. Biophys. Res. Commun. 492, 643–651.
Oh, Y., Zhang, F., Wang, Y., Lee, E.M., Choi, I.Y., Lim, H., Mirakhori, F., Li, R., Huang, L., Xu, T., Wu, H., Li, C., Qin, C.F., Wen, Z., Wu, Q.F., Tang, H., Xu, Z., Jin, P., Song, H., Ming, G.L., Lee, G., 2017. Zika virus directly infects peripheral neurons and induces cell death. Nat. Neurosci. 20, 1209–1212.
Robaszkiewicz, A., Erdelyi, K., Kovacs, K., Kovacs, I., Bai, P., Rajnavolgyi, E., Virag, L., 2012. Hydrogen peroxide-induced poly(ADP-ribosyl)ation regulates osteogenic differentiation-associated cell death. Free Radic. Biol. Med. 53, 1552–1564.
Sarno, M., Sacramento, G.A., Khouri, R., do Rosario, M.S., Costa, F., Archanjo, G., Santos, L.A., Nery Jr., N., Vasilakis, N., Ko, A.I., de Almeida, A.R., 2016. Zika virus infection and stillbirths: a case of hydrops fetalis, hydranencephaly and fetal demise. PLoS Neglected Trop. Dis. 10, e0004517.
Saw, W.G., Pan, A., Subramanian Manimekalai, M.S., Gruber, G., 2017. Structural features of Zika virus non-structural proteins 3 and -5 and its individual domains in solution as well as insights into NS3 inhibition. Antivir. Res. 141, 73–90.
Shi, J., Gao, W., Shao, F., 2017. Pyroptosis: gasdermin-mediated programmed necrotic cell death. Trends Biochem. Sci. 42, 245–254.
Shieh, W.M., Ame, J.C., Wilson, M.V., Wang, Z.Q., Koh, D.W., Jacobson, M.K., Jacobson, E.L., 1998. Poly(ADP-ribose) polymerase null mouse cells synthesize ADP-ribose polymers. J. Biol. Chem. 273, 30069–30072.
Simpson, D.I., 1964. Zika virus infection in man. Trans. R. Soc. Trop. Med. Hyg. 58, 335–338.
Upton, J.W., Chan, F.K., 2014. Staying alive: cell death in antiviral immunity. Mol. Cell 54, 273–280.
Ventura, C.V., Maia, M., Bravo-Filho, V., Gois, A.L., Belfort Jr., R., 2016. Zika virus in Brazil and macular atrophy in a child with microcephaly. Lancet 387, 228.
Virag, L., Robaszkiewicz, A., Rodriguez-Vargas, J.M., Oliver, F.J., 2013. Poly(ADP-ribose) signaling in cell death. Mol. Asp. Med. 34, 1153–1167.
Wang, Y., An, R., Umanah, G.K., Park, H., Nambiar, K., Eacker, S.M., Kim, B., Bao, L., Harraz, M.M., Chang, C., Chen, R., Wang, J.E., Kam, T.I., Jeong, J.S., Xie, Z., Neifert, S., Qian, J., Andrabi, S.A., Blackshaw, S., Zhu, H., Song, H., Ming, G.L., Dawson, V.L., Dawson, T.M., 2016. A nuclease that mediates cell death induced by DNA damage and poly(ADP-ribose) polymerase-1. Science 354.
Wang, Y., Dawson, V.L., Dawson, T.M., 2009. Poly(ADP-ribose) signals to mitochondrial AIF: a key event in parthanatos. Exp. Neurol. 218, 193–202.
Wikan, N., Smith, D.R., 2016. Zika virus: history of a newly emerging arbovirus. Lancet Infect. Dis. 16, e119–e126.
Yu, S.W., Andrabi, S.A., Wang, H., Kim, N.S., Poirier, G.G., Dawson, T.M., Dawson, V.L., 2006. Apoptosis-inducing factor mediates poly(ADP-ribose) (PAR) polymer-induced cell death. Proc. Natl. Acad. Sci. U. S. A. 103, 18314–18319.
Yu, S.W., Wang, H., Poitras, M.F., Coombs, C., Bowers, W.J., Federoff, H.J., Poirier, G.G., Dawson, T.M., Dawson, V.L., 2002. Mediation of poly(ADP-ribose) polymerase-1-dependent cell death by apoptosis-inducing factor. Science 297, 259–263.
Yuan, S., Chu, H., Zhao, H., Zhang, K., Singh, K., Chow, B.K., Kao, R.Y., Zhou, J., Zheng, B.J., 2016. Identification of a small-molecule inhibitor of influenza virus via disrupting the subunits interaction of the viral polymerase. Antivir. Res. 125, 34–42.
Zanluca, C., Dos Santos, C.N., 2016. Zika virus - an overview. Microb. Infect. 18, 295–301.